

Fig. 4. Bim1p recruits Kar9p onto microtubules in vitro. (A) his₇-Bim1p microtubule-binding experiment; (B) [³⁵S]Kar9p microtubule-binding experiment; (C) Experiment containing both his₇-Bim1p and [³⁵S]Kar9p; (D) Experiment containing [³⁵S]Kar9p and recombinant Ase1p. (+) indicates experiments with taxol-stabilized bovine microtubules; (-) indicates experiments without tubulin. s, supernatant; p, pellet. Greater than 80% of the tubulin fractionated into the pellet in the microtubule-binding assays as demonstrated by Coomassie Brilliant Blue stained gels. In the microtubule-binding assays, the concentration of tubulin was 1 μM and the concentration of his₇-Bim1p and Ase1p was 100 nM. Methods of Bim1p purification, Ase1p purification, and the microtubule-binding assay are as described (23, 37).

ordinate spindle or centrosome positioning with cell migration. Chromosomal instability, a hallmark of colon cancer, might also be accelerated by loss of the EB1-APC interaction.

Note added in proof: Similar results are reported in two independent studies (38, 39).

References and Notes

1. T. J. Mitchison and M. W. Kirschner, *J. Cell Biol.* **101**, 766 (1985).
2. A. A. Hyman, *J. Cell Biol.* **109**, 1185 (1989).
3. M. S. Rhyu and J. A. Knoblich, *Cell* **82**, 523 (1995).
4. M. Snyder, S. Gehrung, B. D. Page, *J. Cell Biol.* **114**, 515 (1991).
5. A. J. Hunt and J. R. McIntosh, *Mol. Biol. Cell* **9**, 2857 (1998).
6. E. Fuchs and Y. Yang, *Cell* **98**, 547 (1999).
7. J. Chant and J. R. Pringle, *Curr. Opin. Genet. Dev.* **1**, 342 (1991).
8. S. L. Shaw *et al.*, *Mol. Biol. Cell* **9**, 1627 (1998).
9. R. H. Gavin, *Int. Rev. Cytol.* **173**, 207 (1997).
10. R. A. Heil-Chapdelaine, N. R. Adames, J. A. Cooper, *J. Cell Biol.* **144**, 809 (1999).
11. S. Busson, D. Dujardin, A. Moreau, J. Dompierre, J. R. DeMay, *Curr. Biol.* **8**, 541 (1998).
12. X. Xiang, C. Roghi, N. R. Morris, *Proc. Natl. Acad. Sci. U.S.A.* **92**, 9890 (1995).

13. P. Gonczy, S. Pihchler, M. Kirkham, A. A. Hyman, *J. Cell Biol.* **147**, 135 (1999).
14. T. DeZwaan, E. Ellingson, D. Pellman, D. M. Roof, *J. Cell Biol.* **138**, 1023 (1997).
15. F. R. Cottingham and M. A. Hoyt, *J. Cell Biol.* **138**, 1041 (1997).
16. R. K. Miller *et al.*, *Mol. Biol. Cell* **9**, 2051 (1998).
17. L. Lee, S. K. Klee, M. Evangelista, C. Boone, D. Pellman, *J. Cell Biol.* **144**, 947 (1999).
18. M. Evangelista *et al.*, *Science* **276**, 118 (1997).
19. R. K. Miller and M. D. Rose, *J. Cell Biol.* **140**, 377 (1998).
20. R. K. Miller, D. Matheos, M. D. Rose, *J. Cell Biol.* **144**, 963 (1999).
21. J. S. Tirnauer, E. O'Toole, L. Berrueta, B. E. Bierer, D. Pellman, *J. Cell Biol.* **145**, 993 (1999).
22. L. Lee, J. Y. Liu, D. Pellman, unpublished data.
23. Supplemental material is available at www.sciencemag.org/feature/data/1047337.shl
24. J. P. Juwana *et al.*, *Int. J. Cancer* **81**, 275 (1999).
25. L. Berrueta *et al.*, *Proc. Natl. Acad. Sci. U.S.A.* **95**, 10596 (1998).
26. H. Imamura *et al.*, *EMBO J.* **16**, 2745 (1997).
27. L. Muhua, N. R. Adames, M. D. Murphy, C. R. Shields, J. A. Cooper, *Nature* **393**, 487 (1998).
28. The delivery of Bim1p to cortical Kar9p binding sites could signal the successful completion of spindle positioning and promote cytokinesis on schedule. However, we found that Kar9p was not required for the cytokinesis checkpoint (L. Lee and D. Pellman, unpublished data).
29. E. E. Morrison, B. N. Wardleworth, J. M. Askham, A. F. Markham, D. M. Meredith, *Oncogene* **17**, 3471 (1998).
30. L.-K. Su *et al.*, *Cancer Res.* **55**, 2972 (1995).
31. G. G. Gundersen and T. A. Cook, *Curr. Opin. Cell Biol.* **11**, 81 (1999).
32. K. Schwartz, K. Richards, D. Botstein, *Mol. Biol. Cell* **8**, 2677 (1997).
33. An astral microtubule was considered correctly oriented if it extended into the bud or mating projection. Analysis was limited to microtubules of length equal to or greater than the shortest distance from the centrosome to the GFP-Kar9p signal. The percentage of preanaphase cells that met the above

criteria was 89% in the *BIM1* strain ($n = 100$) and 8% in the *bim1Δ* strain ($n = 228$). In α factor-arrested cells, the percentage was 89% in the *BIM1* strain ($n = 141$) and 27% in the *bim1Δ* strain ($n = 321$). It is likely that misoriented microtubules in *bim1Δ* cells are misoriented because they fail to interact with Kar9p. If this is the case, then Bim1p is required for microtubule ends to interact with Kar9p in most cells.

34. Cell extracts for Western analysis and immunoprecipitations were prepared by glass bead lysis in a buffer containing 150 mM NaCl, 50 mM Tris (pH 8.0), 1% Nonidet P-40, and protease inhibitors. Antibodies for immunoblotting: HA-Bim1p was detected with 12CA5, GFP-Kar9p was detected with a polyclonal antibody to GFP, and tubulin was detected with a monoclonal antibody to α tubulin.
35. Sucrose gradients (5 to 20%) were made in 50 mM Tris (pH 8.0) and 150 mM NaCl. We loaded 400 μl of low-speed supernatant on top of each 12.5-ml gradient and spun it overnight in a Beckman SW40 Ti at 218,000g. The linearity of the gradients was confirmed by refractometry, and Svedberg values were calculated on the basis of globular standards. Gel filtration was performed using a Bio-Rad SE-1000 analytical Gel Filtration column.
36. L. M. Siegel and K. J. Monty, *Biochim. Biophys. Acta* **112**, 346 (1966).
37. K. A. Butner and M. W. Kirschner, *J. Cell Biol.* **115**, 717 (1991).
38. W. S. Korinek, M. J. Copeland, A. Chaudhuri, J. Chant, *Science* **287**, 2257 (2000).
39. R. K. Miller, S.-C. Cheng, M. D. Rose, in preparation.
40. We thank J. DeCaprio, E. Elion, J. Kahana, R. Miller, M. Rose, and P. Silver for reagents, E. Elion, R. Li, T. Look, and M. McLaughlin for comments on the manuscript, J. Chant and M. Rose for communicating results before publication, and B. Bierer and members of the Pellman laboratory for discussions. Supported by grants from NIH [GM55772 to D.P. and KO8 DK02578 to J.S.T.] and a Kimmel Scholar Award to D.P.

23 November 1999; accepted 15 February 2000

Driving AMPA Receptors into Synapses by LTP and CaMKII: Requirement for GluR1 and PDZ Domain Interaction

Yasunori Hayashi,* Song-Hai Shi,* José A. Esteban, Antonella Piccini, Jean-Christophe Poncer,† Roberto Malinow‡

To elucidate mechanisms that control and execute activity-dependent synaptic plasticity, α-amino-3-hydroxy-5-methyl-4-isoxazole propionate receptors (AMPA-Rs) with an electrophysiological tag were expressed in rat hippocampal neurons. Long-term potentiation (LTP) or increased activity of the calcium/calmodulin-dependent protein kinase II (CaMKII) induced delivery of tagged AMPA-Rs into synapses. This effect was not diminished by mutating the CaMKII phosphorylation site on the GluR1 AMPA-R subunit, but was blocked by mutating a predicted PDZ domain interaction site. These results show that LTP and CaMKII activity drive AMPA-Rs to synapses by a mechanism that requires the association between GluR1 and a PDZ domain protein.

Long-term potentiation (LTP) of synaptic transmission is a well-characterized form of activity-dependent plasticity likely to play important roles in learning and memory (1). A key mediator of this plasticity is CaMKII, an enzyme that

is strongly expressed at excitatory synapses (2). Although the cell biological processes underlying this form of plasticity are poorly understood, the trafficking of synaptic receptors appears to play a crucial role (3).

REPORTS

Genes of interest were delivered to neurons in organotypically cultured hippocampal slices, using the Sindbis virus expression system (3–5). Neurons carrying foreign genes were identified by green fluorescent protein (GFP) expression and whole-cell recordings were obtained (Fig. 1A) (6). To examine the effect of elevated CaMKII activity on neuronal function, we generated a construct encoding the catalytic domain of this enzyme fused with GFP (tCaMKII-GFP). The expression of this construct increased constitutive CaMKII activity in baby hamster kidney (BHK) cells (Fig. 1B) (7). In hippocampal slice neurons expressing this construct, fluorescence was detected in dendritic arbors and spines (8). To determine the effect on synaptic transmission, we measured synaptic responses in two nearby neurons, one infected with tCaMKII-GFP (indicated by GFP fluorescence) and the other uninfected (Fig. 1, A and D). Such pairwise comparisons of synaptic responses to stimuli delivered at the same site showed that tCaMKII-GFP enhanced transmission (Fig. 1D) (9–11). Cells infected with GFP alone did not show any change in synaptic response (Fig. 1C).

To examine if this increase in AMPA-R-mediated transmission was due to a delivery of receptors to synapses, we developed an electrophysiological assay. The current-voltage (*I-V*) relationship of AMPA-Rs is determined by the GluR2 subunit: AMPA-Rs with GluR2 show linear *I-V* relations; AMPA-Rs lacking GluR2 show little outward current at +40 mV (12). Most AMPA-Rs in hippocampal pyramidal cells contain the GluR2 subunit (13), consistent with the linear *I-V* relationship of synaptic transmission (14). We overexpressed the AMPA-R GluR1 subunit in hippocampal slice neurons (Fig. 2A). This protein was tagged with GFP to facilitate identification of expressing neurons and immunoprecipitation (3). As demonstrated by coimmunoprecipitation experiments, most of the resulting recombinant AMPA-Rs lacked GluR2 (Fig. 2B) (15). Such receptors were functional and showed complete inward rectification when expressed in HEK293 cells (3). Thus, incorporation of these recombinant receptors into synapses would be expected to increase rectification of synaptic responses (16).

GluR1-GFP is widely distributed throughout the dendritic arbor, but little is incorporated into synapses in the absence of activity (3). In agreement with this, expression of

GluR1-GFP had no effect on either the amplitude or rectification of synaptic transmission (Fig. 2C). To determine if CaMKII activity could drive the recombinant GluR1-GFP into synapses, we coexpressed GluR1-GFP and tCaMKII by using an internal ribosomal entry site (IRES) construct (5, 17). BHK cells expressing this construct showed

increased constitutive CaMKII activity (Fig. 1B) (7), and slices expressing this construct showed fluorescence (indicating GluR1-GFP expression) (8). Pairwise recordings from infected and noninfected cells showed that transmission was enhanced (Fig. 2D), consistent with an increase of CaMKII activity (10, 18). Notably, transmission showed increased

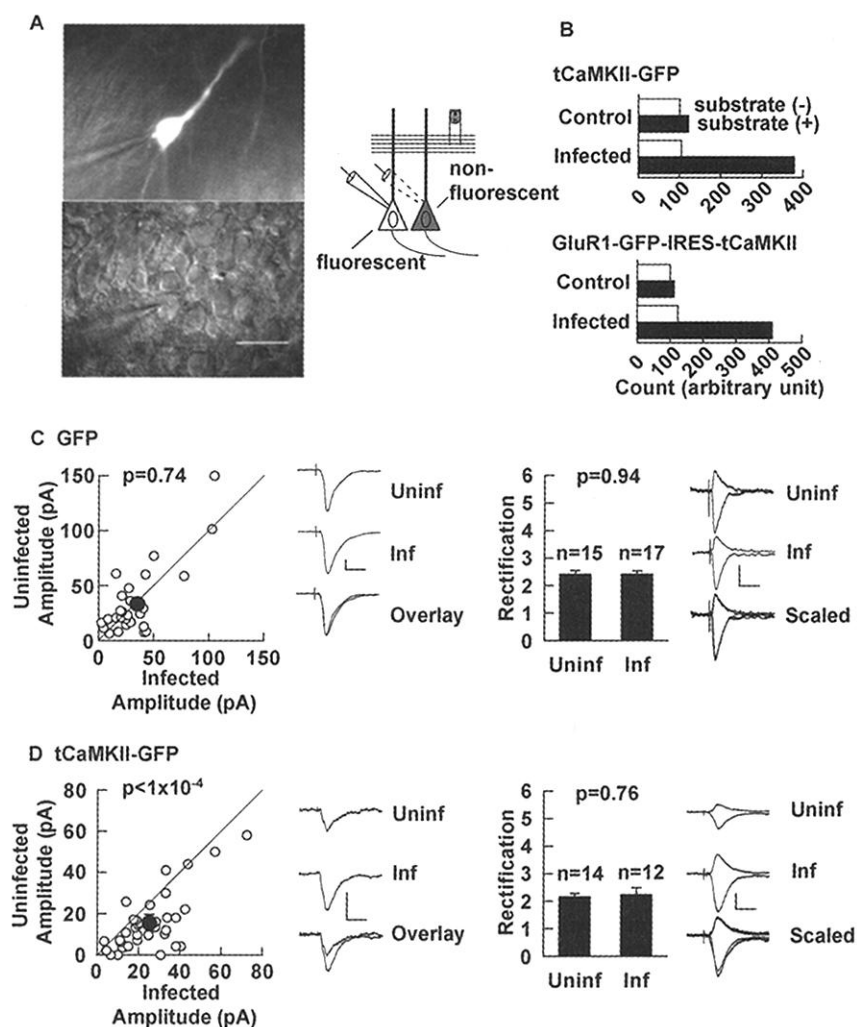


Fig. 1. Enhanced synaptic transmission in neurons expressing tCaMKII-GFP. **(A)** Hippocampal CA1 pyramidal neuron infected with Sindbis virus and expressing GFP. Fluorescent (top) and differential interference contrast (bottom) images of the same field during electrophysiological recording. Bar: 30 μ m. Schematic diagram on right: Whole-cell recordings were obtained from a fluorescent (infected) and an adjacent nonfluorescent (uninfected) neuron with identical stimulation position and intensity. **(B)** Calcium/calmodulin-independent kinase activity of tCaMKII constructs. BHK cells were infected with respective Sindbis viruses, and Ca^{2+} /calmodulin-independent kinase activity was determined. Controls were uninfected cells (top) or lacZ-infected cells (bottom). **(C)** Synaptic responses from neurons expressing GFP or from nearby nonexpressing cells. (Left panel) For each pair of cells, the amplitude of response from infected cell is plotted against amplitude of response in uninfected cell ($n = 27$). Mean of all values is shown in filled circle (uninfected: 35.1 ± 6.3 ; infected: 33.4 ± 5.0). (Right panel) Summary results of measured rectification for uninfected (2.4 ± 0.1 , $n = 15$) and infected (2.4 ± 0.1 , $n = 17$) cells. Sample responses from nearby uninfected and infected cells are overlaid and shown on right side of each panel. For rectification, responses were obtained at -60 and $+40$ mV; responses from infected and uninfected cells are not necessarily from nearby cells. Scaled: responses from uninfected cell were scaled so that the current at $+40$ mV matched that of the infected cell. Bars: 20 pA, 25 ms. Same symbols, trace display conventions, and bar values are used in subsequent figures. **(D)** tCaMKII-GFP produces enhancement of synaptic transmission in expressing neurons (left panel: uninfected: 15.4 ± 2.4 ; infected: 25.3 ± 2.5 , $n = 35$) with no effect on rectification (right panel: 2.2 ± 0.1 , $n = 14$ for uninfected and 2.2 ± 0.3 , $n = 12$ for infected cells).

Cold Spring Harbor Laboratory, Cold Spring Harbor, NY 11724, USA.

*These authors contributed equally to this work.

†Present address: INSERM U261, Institut Pasteur, 25 rue du Dr. Roux, 75015 Paris, France.

‡To whom correspondence should be addressed. E-mail: malinow@cshl.org

REPORTS

rectification, indicating a contribution of the homomeric GluR1-GFP to transmission (Fig. 2D). This effect on rectification was due to coexpression of the two proteins, because transmission onto cells expressing either tCaMKII or GluR1-GFP alone had rectification comparable to that in uninfected cells (Figs. 1D and 2C). These results show that CaMKII activity induces the insertion of homomeric GluR1-GFP into the synapse.

GluR1 is phosphorylated by CaMKII at Ser⁸³¹ during LTP (19). To examine if direct phosphorylation of the receptor at this site is required for delivery, we substituted Ser⁸³¹ with Ala, thus creating GluR1(S831A)-GFP (Fig. 3, A and B). This mutation, however, did not block delivery. Expression of this construct alone changed neither amplitude nor rectification (Fig. 3C), and coexpression with tCaMKII produced potentiated transmission that showed the same increase in rectification as that seen with GluR1-GFP-IRES-tCaMKII (Fig. 3D).

The subcellular localization of many membrane proteins is controlled by associations with a class of proteins containing PDZ domains (20). (The name PDZ derives from the proteins PSD-95, Dlg, and ZO1, which contain the domain.) In particular, the very COOH-terminus of the cytosolic tail of such surface proteins has a consensus (S/T)X(V/L) (20, 21). Serine or threonine at -2 position appears to be crucial because a mutation at this site can prevent associations (20). The last three amino acids of the COOH-terminus of GluR1 are TGL, which conforms to the consensus sequence. We converted the GluR1 COOH-terminus from TGL to AGL, thus creating GluR1(T887A)-GFP (Fig. 3A). This protein, when expressed in HEK293 cells, formed functional AMPA-Rs that showed the normal rectification (Fig. 3B). When expressed in hippocampal neurons, this protein was detected in dendrites (8). This construct showed no effect on transmission when expressed alone (Fig. 3E). However, when GluR1(T887A)-GFP and tCaMKII were coexpressed in hippocampal slice neurons, the effects of tCaMKII on synaptic response amplitude and rectification were completely blocked. Indeed, transmission onto these neurons was depressed (Fig. 3F).

To determine if LTP delivers AMPA-Rs to synapses through a similar mechanism, we examined LTP in cells expressing GluR1-GFP. Whole-cell recordings were obtained from cells expressing (Fig. 4A, top) or not expressing (Fig. 4A, bottom) GluR1-GFP. LTP was induced with a pairing protocol (6). We added DL-2-amino-5-phosphonovaleric acid (APV) to the bath 30 min after potentiated transmission was measured, in order to isolate pure AMPA-R-mediated responses. The holding membrane potential was then switched to measure rectification of the

AMPA-R-mediated responses. Similar to the effect of coexpressed CaMKII and GluR1-GFP, rectification was increased after LTP in cells expressing GluR1-GFP (4.6 ± 0.7 ; $n = 14$) compared to cells not expressing GluR1-GFP (2.7 ± 0.2 ; $n = 15$) (Fig. 4B). In 5 of the 14 experiments on cells expressing GluR1-GFP, a control (nonpaired) pathway was monitored, and rectification in this pathway was not increased (Fig. 4B).

We also examined the effects of GluR1(T887A) on LTP. As shown above, this receptor, which has the PDZ-interaction site mutated, can completely block the potentiation produced by tCaMKII. In a series of

blind experiments, we recorded synaptic responses from cells expressing either GluR1-GFP or GluR1(T887A)-GFP. After pairing, cells expressing the control construct displayed stable potentiation lasting at least 50 min, at which time the recording was terminated (Fig. 4C, top, and Fig. 4D, top). Cells expressing GluR1(T887A)-GFP displayed a very different response. After a pairing protocol, these cells showed a short-lasting potentiation that decayed over the next 20 min; 45 min after pairing, the responses were significantly depressed from baseline levels (Fig. 4C, bottom, and Fig. 4D, top). In 4 of the 21 experiments with GluR1(T887A), a

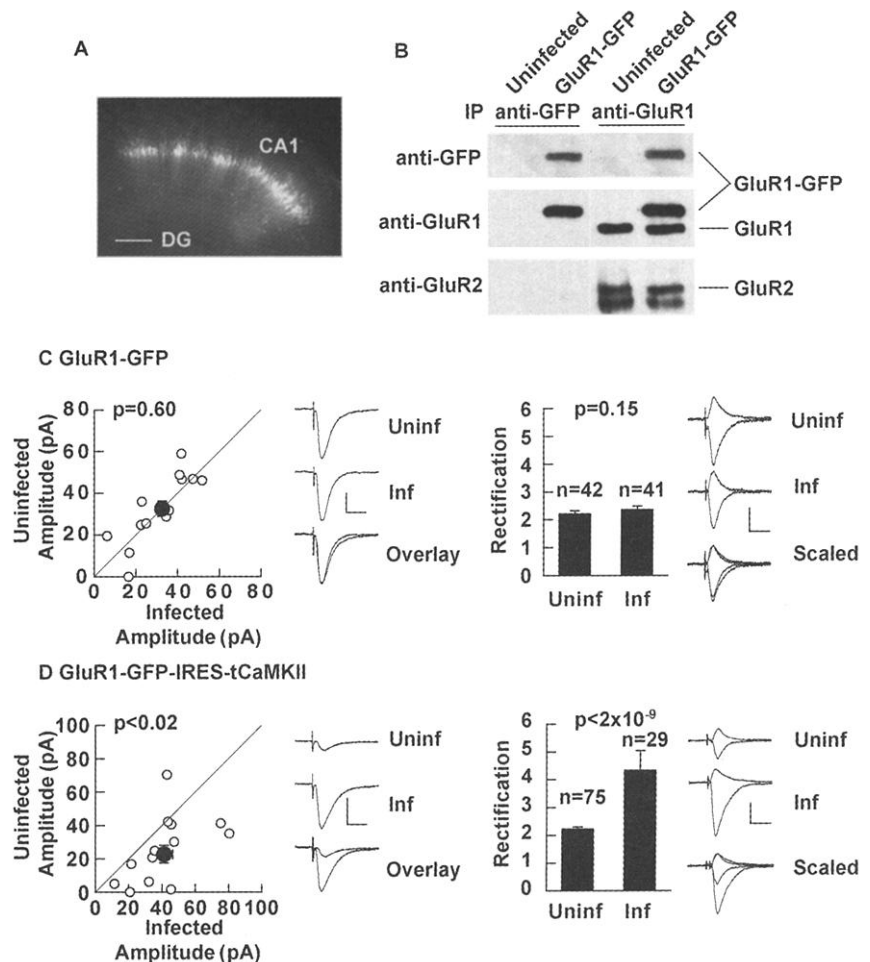


Fig. 2. Increased CaMKII activity delivers GluR1-GFP into synapses. **(A)** Fluorescence image of a hippocampal slice expressing GluR1-GFP. Sindbis virus particles expressing GluR1-GFP were injected into several sites of CA1 pyramidal cell layer. DG, dentate gyrus. Bar: 300 μ m. **(B)** Immunoprecipitation study indicates that GluR1-GFP forms largely homomers. GluR1-GFP was immunoprecipitated from hippocampal slices with anti-GFP (two left lanes) or anti-GluR1 (two right lanes) and blotted with anti-GFP (top), anti-GluR1 (middle), and anti-GluR2 (bottom). GluR2 immunoreactivity did not coprecipitate with GFP immunoreactivity. In contrast, GluR2 coprecipitated with endogenous GluR1, indicating coimmunoprecipitation itself was successful. The lower bands observed in the GluR2 blot derive from antibody used for immunoprecipitation. **(C)** Synaptic responses from neurons expressing GluR1-GFP and nearby nonexpressing cells. Expression of GluR1-GFP did not affect the amplitude (uninfected: 32.7 ± 4.1 ; infected: 31.0 ± 3.3 , $n = 13$) or rectification (2.2 ± 0.1 , $n = 42$ for uninfected; 2.4 ± 0.1 , $n = 41$ for infected cells). **(D)** Coexpression of GluR1-GFP with tCaMKII increased amplitude (uninfected: 25.7 ± 5.3 ; infected: 41.3 ± 5.1 , $n = 13$) and rectification (2.2 ± 0.4 , $n = 75$ for uninfected; 4.3 ± 0.7 , $n = 29$ for infected cells).

control (nonpaired) pathway was monitored, which did not show depression (Fig. 4D, top).

The cell-biological mechanisms underlying synaptic plasticity have been difficult to delineate. In part, this is due to the lack of techniques in intact preparations allowing molecular perturbations with spatial and temporal control, as well as the absence of assays for specific molecular events linked to synaptic plasticity. Here, we generated electrophysiologically tagged receptors to monitor their synaptic delivery during LTP and increased CaMKII. In the absence of plasticity-inducing stimuli, we saw no evidence for

their contribution to transmission. This is consistent with previous results indicating that in the absence of evoked activity, GluR1 is retained within the dendrite (3). Upon coexpression with constitutively active CaMKII or following LTP induction, we see that tagged receptors contribute to transmission, indicating their delivery to synapses.

Previous studies indicate that LTP induction increases the CaMKII-dependent phosphorylation of GluR1 at Ser⁸³¹ (19). Although such phosphorylation may enhance the function of synaptic receptors (22), this phosphorylation does not seem to be required

for receptor delivery: tCaMKII can deliver GluR1(S831A)-GFP to the synapse (23). Our results indicate that some protein(s) other than GluR1 must be substrate(s) of CaMKII and participate in the regulated delivery of AMPA-Rs.

The most surprising of our results relate to the effects of GluR1(T887A). This protein forms functional receptors and has no detectable effects on basal synaptic transmission. However, this mutant receptor can block the effects of tCaMKII and LTP (24). This has several implications: (i) It reinforces the view that CaMKII and LTP act through similar mechanisms. (ii) It indicates that both CaMKII-potentiation and LTP exert their effects through GluR1. (iii) It indicates that an interaction between GluR1 and a protein with a PDZ domain plays a key intermediate in these forms of plasticity. (iv) GluR1(T887A) depresses transmission, but only after increased CaMKII or LTP. This last finding suggests that activity enables the mutant protein to interrupt a constitutive delivery of endogenous AMPA-Rs (25).

These results demonstrate that incorporation of GluR1-containing AMPA-Rs into synapses is a major mechanism underlying the plasticity produced by activation of CaMKII and LTP. This process requires phosphorylation of protein(s) other than GluR1. Furthermore, this delivery requires interactions between the COOH-terminus of GluR1 and PDZ domain proteins.

References and Notes

1. T. V. P. Bliss and G. L. Collingridge, *Nature* **361**, 31 (1993).
2. S. G. Miller and M. B. Kennedy, *J. Biol. Chem.* **260**, 9039 (1985); P. T. Kelly, T. L. McGuinness, P. Greengard, *Proc. Natl. Acad. Sci. U.S.A.* **81**, 945 (1984); R. Malinow, H. Schulman, R. W. Tsien, *Science* **245**, 862 (1989); R. C. Malenka et al., *Nature* **340**, 554 (1989); A. J. Silva, C. F. Stevens, S. Tonegawa, Y. Wang, *Science* **257**, 201 (1992); A. P. Braun and H. Schulman, *Annu. Rev. Physiol.* **57**, 417 (1995); J. Lisman, R. C. Malenka, R. A. Nicoll, R. Malinow, *Science* **276**, 2001 (1997); G.-Y. Wu and H. T. Cline, *Science* **279**, 222 (1998).
3. S.-H. Shi et al., *Science* **284**, 1811 (1999).
4. R. Malinow et al., in *Imaging Living Cells*, R. Yuste, A. Lanni, A. Konnerth, Eds. (Cold Spring Harbor Laboratory Press, Cold Spring Harbor, NY, 1999), pp. 58-1-58-9.
5. Construction of GluR1-GFP was described in (3). Point mutants of GluR1-GFP were generated by QuickChange mutagenesis kit (Stratagene). CaMKII cDNA was isolated from a rat forebrain cDNA library, mutated so that initiation methionine overlaps the Nco I site (ccATGg), and truncated after the 290th amino acid by adding a stop codon. This truncated CaMKII (tCaMKII) cDNA was cloned after the IRES sequence derived from encephalomyocarditis virus so that the initiation methionine matches the 12th ATG of IRES. The resulting IRES-tCaMKII was transferred downstream to GluR1-GFP mutant constructs. The tCaMKII-GFP fusion protein construct was made by inserting polymerase chain reaction-amplified tCaMKII fragment into pEGFP-N1 vector (Clontech). Sindbis virus containing each of these constructs was produced as described (3, 4).
6. Electrophysiological recordings from CA1 pyramidal neurons were carried out in rat hippocampal organotypic slice cultures prepared as described (3). Neurons were infected as described (3), and recordings were made 24 to 36 hours later. External solution

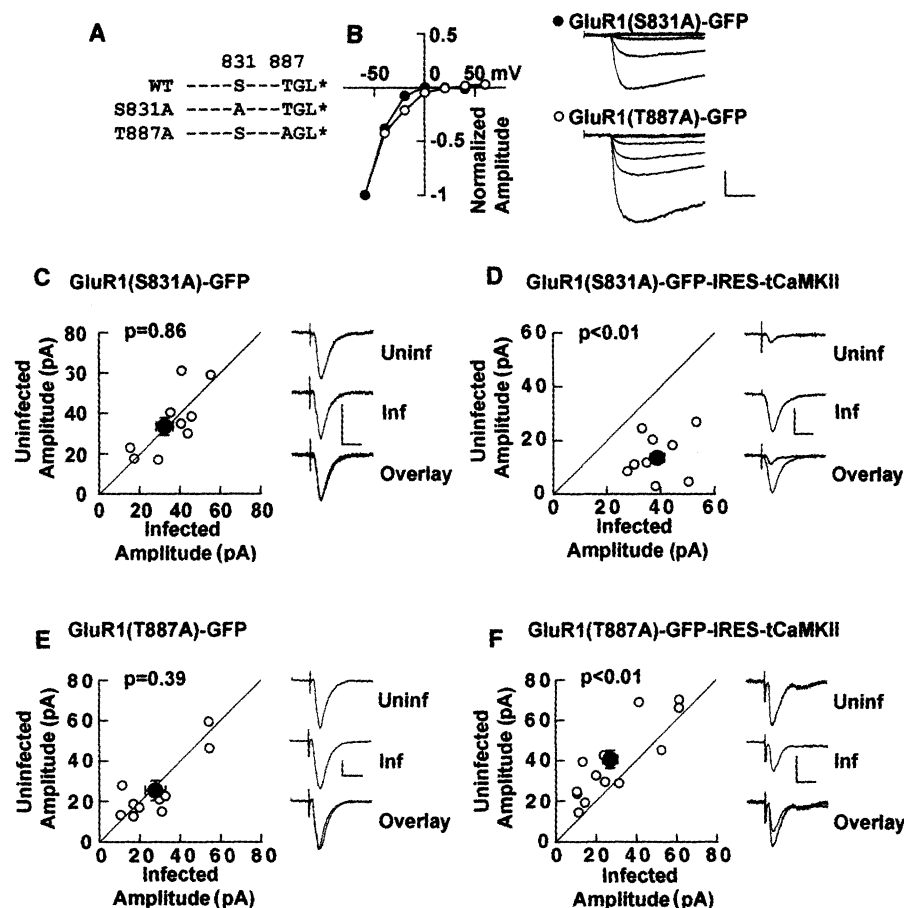


Fig. 3. CaMKII-driven delivery of GluR1 to synapses is not dependent on phosphorylation at Ser⁸³¹ but on interaction with putative PDZ domain protein. (A) COOH-terminus of GluR1 wild-type (WT) and two point mutants used in this study. Asterisks indicate stop codon. (B) Current-voltage relationship of current evoked by kainate (1 mM) onto HEK cells expressing GluR1(S831A)-GFP (filled circles, $n = 3$) and GluR1(T887A)-GFP (open circles, $n = 3$). Responses were recorded at -60 to $+40$ mV (in 20-mV steps) and are normalized by the response at -60 mV. Sample traces are shown on right. Bar: 50 pA, 200 ms. (C) GluR1(S831A)-GFP alone did not have any effect on either amplitude (uninfected: 35.8 ± 4.5 ; infected: 36.0 ± 3.7 , $n = 9$) or rectification (2.4 ± 0.3 , $n = 14$ for uninfected cells; 2.3 ± 0.3 , $n = 16$ for infected cells, $P = 0.55$; see Web figure 2). (D) Coexpression of tCaMKII and GluR1(S831A)-GFP resulted in increased amplitude (uninfected: 14.4 ± 2.6 ; infected: 38.7 ± 2.7 , $n = 9$) and rectification (2.1 ± 0.1 , $n = 36$ for uninfected cells; 3.6 ± 0.2 , $n = 15$ for infected cells, $P < 10^{-6}$; see Web figure 2) indicating that receptor delivery is not dependent on the phosphorylation of the receptor at Ser⁸³¹. (E) Expression of GluR1(T887A)-GFP had no effect on synaptic amplitude (uninfected: 25.5 ± 4.9 ; infected: 27.7 ± 5.1 , $n = 10$) or rectification (2.2 ± 0.2 , $n = 14$ for uninfected cells; 2.4 ± 0.2 , $n = 11$ for infected cells, $P = 0.51$; see Web figure 2). (F) Coexpression of GluR1(T887A)-GFP with tCaMKII blocked potentiation by tCaMKII. Coexpression resulted in depressed transmission (infected: 28.9 ± 4.3 ; uninfected: 38.9 ± 4.2 , $n = 13$) with no change in rectification (2.2 ± 0.1 , $n = 36$ for uninfected cells; 2.4 ± 0.2 , $n = 15$ for infected cells, $P = 0.73$; see Web figure 2).

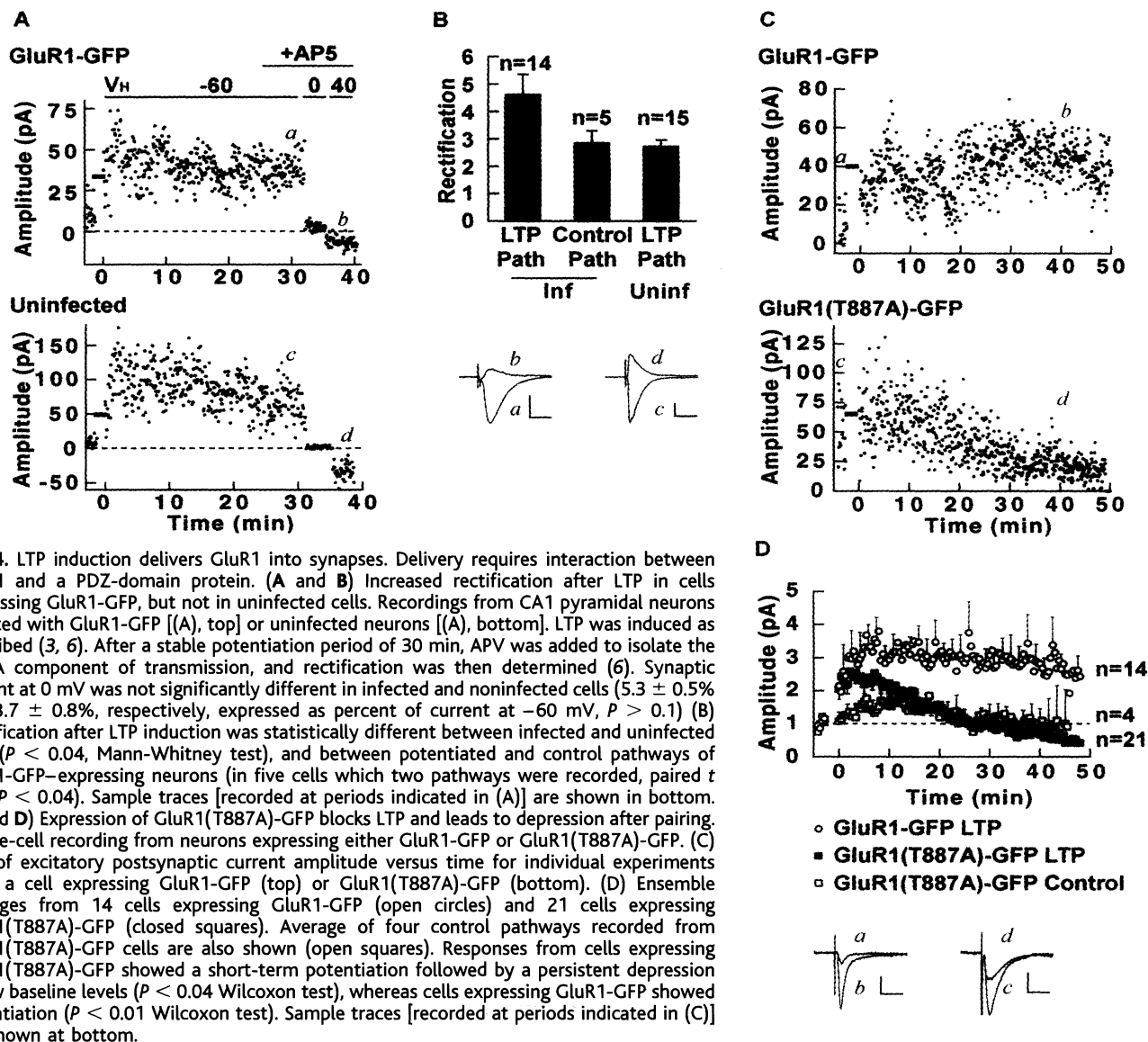


Fig. 4. LTP induction delivers GluR1 into synapses. Delivery requires interaction between GluR1 and a PDZ-domain protein. (A and B) Increased rectification after LTP in cells expressing GluR1-GFP, but not in uninfected cells. Recordings from CA1 pyramidal neurons infected with GluR1-GFP [(A), top] or uninfected neurons [(A), bottom]. LTP was induced as described (3, 6). After a stable potentiation period of 30 min, APV was added to isolate the AMPA component of transmission, and rectification was then determined (6). Synaptic current at 0 mV was not significantly different in infected and noninfected cells ($5.3 \pm 0.5\%$ and $3.7 \pm 0.8\%$, respectively, expressed as percent of current at -60 mV, $P > 0.1$) (B) Rectification after LTP induction was statistically different between infected and uninfected cells ($P < 0.04$, Mann-Whitney test), and between potentiated and control pathways of GluR1-GFP-expressing neurons (in five cells which two pathways were recorded, paired t test, $P < 0.04$). Sample traces [recorded at periods indicated in (A)] are shown in bottom. (C and D) Expression of GluR1(T887A)-GFP blocks LTP and leads to depression after pairing. Whole-cell recording from neurons expressing either GluR1-GFP or GluR1(T887A)-GFP. (C) Plot of excitatory postsynaptic current amplitude versus time for individual experiments from a cell expressing GluR1-GFP (top) or GluR1(T887A)-GFP (bottom). (D) Ensemble averages from 14 cells expressing GluR1-GFP (open circles) and 21 cells expressing GluR1(T887A)-GFP (closed squares). Average of four control pathways recorded from GluR1(T887A)-GFP cells are also shown (open squares). Responses from cells expressing GluR1(T887A)-GFP showed a short-term potentiation followed by a persistent depression below baseline levels ($P < 0.04$ Wilcoxon test), whereas cells expressing GluR1-GFP showed potentiation ($P < 0.01$ Wilcoxon test). Sample traces [recorded at periods indicated in (C)] are shown at bottom.

contained 119 mM NaCl, 2.5 mM KCl, 2 mM CaCl₂, 4 mM MgCl₂, 26.2 mM NaHCO₃, 1 mM NaH₂PO₄, 11 mM glucose, 100 μM picrotoxin, 20 μM bicuculline, 100 μM APV, 1 μM 3-((R,S)-2-carboxypiperazin-4-yl)-propyl-1-phosphonic acid (CPP), and 4 to 10 μM 2-chloroadenosine (to reduce polysynaptic excitation) and was gassed with 5% CO₂ and 95% O₂ at ambient temperature. Internal solution consisted of 115 mM cesium methanesulfonate, 20 mM CsCl, 10 mM HEPES, 2.5 mM MgCl₂, 4 mM Na₂-ATP (adenosine triphosphate), 0.4 mM Na-GTP (guanosine triphosphate), 10 mM sodium phosphocreatine, 0.6 mM EGTA, and 0.1 mM spermine (pH 7.2). For recordings from cell pairs, two cells with cell bodies within ~20 μm were selected, one cell showing and the other not showing GFP fluorescence. The stimulus electrode was placed in stratum radiatum, ~50 μm from stratum pyramidale. Recordings were first generally made from an infected cell, and the stimulus level was set to produce a synaptic response of ~30 pA. Upon termination of that recording, a whole-cell recording was immediately obtained from the nearby control cell with the same location and intensity of stimulus. Ratio of amplitude of synaptic response at -60 and $+40$ mV (average of 50 to 100 traces each) was used as a measure of rectification throughout this study. Response at 0 mV was also measured to ensure reversal potential of response and quality of voltage clamping. As expected, recti-

fication is independent of the absolute amplitude of the response [Web figure 1 (26)]. Thus, recordings that were not carried out in a paired fashion were also included in the calculation of the average rectification. However, comparisons were restricted to those among cells recorded on the same day. LTP was induced as described in (3). Baseline recordings were limited to about 2 min due to faster washout of LTP in slice culture. Recording from HEK293 cells was carried out as described (3).

7. Six hours after infection with respective virus, BHK cells (2×10^5 cells per 35-mm dish) were solubilized in 50 mM Hepes-NaOH (pH 7.4), 1 mM EGTA, 0.5 mM dithiothreitol, 50 mM NaCl, 10% glycerol, 40 mM NaF, 0.1 mM phenylmethylsulfonyl fluoride (PMSF), 2 μg/ml CLAP (cocktail of chymostatin, leupeptin, pepstatin A, and antipain), and 1% NP40. The Ca²⁺ and calmodulin-independent phosphorylation was determined in a mixture of 2 μg of protein, 10 mM Hepes-NaOH (pH 7.4), 5 mM MgCl₂, 10 mM EGTA, 50 μM [γ -³²P]ATP (Amersham), 20 μM autocalmitide-2 (Calbiochem), 40 mM NaF, and 0.5 mM dithiothreitol in a final volume of 20 μl. The reaction was carried out at 30°C for 4 min, and the mixture was spotted onto P81 phosphocellulose paper. The paper was immediately dropped into 1% phosphoric acid to terminate the reaction. After washing with the same solution three times, the paper was dried and the radioactivity was measured.

8. Y. Hayashi, S.-H. Shi, J. A. Esteban, R. Malinow, unpublished results.

9. For collection and analysis of electrophysiological data in which there was expression of GluR1 and its mutants, the experimenter was blind to the genotype of Sindbis virus vectors. Resultant data were not significantly different from nonblind experiments and thus were pooled. For assessment of statistical significance to the difference in means, we used Wilcoxon nonparametric test (for change in amplitude between a pair of infected and uninfected cells) and the nonpaired version, the Mann-Whitney nonparametric test (for rectification). The two-tailed P values are indicated in each graph. Student's t test on raw data or on log-normalized data gave similar results. Error bars indicate SEM.

10. D. L. Pettit, S. Perlman, R. Malinow, *Science* **266**, 1881 (1994); P. M. Lledo *et al.*, *Proc. Natl. Acad. Sci. U.S.A.* **92**, 11175 (1995); A. M. Shirke and R. Malinow, *J. Neurophysiol.* **78**, 2682 (1997).

11. This increase in AMPA-R-mediated response is not due to change in electrotonic properties caused by morphological change in dendrite, because the NMDA receptor-mediated component was not changed by expression of tCaMKII. In uninfected cells, NMDA current amplitude was 10.0 ± 1.6 pA, whereas in tCaMKII-GFP infected cells, it was 7.5 ± 1.2 pA. The difference was not statistically significant (Mann-Whitney test: $P = 0.28$; t test: $P = 0.21$, $n = 25$ each).

12. T. A. Verdoorn, N. Burnashev, H. Monyer, P. H. Seeburg, B. Sakmann, *Science* **252**, 1715 (1991).

13. R. J. Wenthold, R. S. Petralia, J. Blahos II, A. S. Niedzielski, *J. Neurosci.* **16**, 1982 (1996).

14. S. Hestrin, R. A. Nicoll, D. J. Perkel, P. Sah, *J. Physiol. (London)* **422**, 203 (1990).

15. After 1.5 days of infection, slices were pooled and solubilized in homogenization buffer (100 μ l per slice) composed of 10 mM Hepes-NaOH, 0.5 M NaCl, 10 mM sodium pyrophosphate, 10 mM NaF, 10 mM EDTA, 4 mM EGTA, 0.1 mM PMSF, 2 μ g/ml CLAP, and 1% Triton X-100. The solution was cleared by centrifugation at 10000g for 5 min at 4°C. To supernatant (0.5 mg of protein per 0.5 ml for each reaction), protein G-Sepharose (40 μ l, 50% volume in homogenization buffer) was added to preabsorb nonspecific resin binding, and the solution was again centrifuged at 5000g for 1 min at 4°C. After reaction with antibody to GFP (anti-GFP, monoclonal, 10 μ g per sample, Boehringer Mannheim) or anti-GluR1 (polyclonal, 1 μ g per sample, Chemicon International) at 4°C for 2 hours, the immunocomplex was absorbed onto protein G-Sepharose resin (40 μ l) at 4°C for 2 hours. Finally, the resin was washed three times with homogenization buffer, subjected to SDS-PAGE, and blotted with anti-GFP (polyclonal, Clontech), anti-GluR1, and anti-GluR2 (polyclonal, Chemicon International).

16. R. L. Neve, J. R. Howe, S. Hong, R. G. Kalb, *Neuroscience* **79**, 435 (1997).

17. R. J. Jackson, M. T. Howell, A. Kaminski, *Trends Biochem. Sci.* **15**, 477 (1990).

18. This response was sensitive to 3 μ M NBQX, an AMPA-R antagonist.

19. A. L. Mammen, K. Kameyama, K. W. Roche, R. L. Huganir, *J. Biol. Chem.* **272**, 32528 (1997); A. Barria, D. Muller, V. Derkach, L. C. Griffith, T. R. Soderling, *Science* **276**, 2042 (1997); A. Barria, V. Derkach, T. Soderling, *J. Biol. Chem.* **272**, 32727 (1997).

20. Z. Songyang et al., *Science* **275**, 73 (1997); H. Dong et al., *Nature* **386**, 279 (1997); J. Saras, U. Engstrom, L. J. Gonce, C. H. Heldin, *J. Biol. Chem.* **272**, 20979 (1997); T. Nagano, H. Jourdi, H. Nawa, *J. Biochem.* **124**, 869 (1998); A. S. Leonard, M. A. Davare, M. C. Horne, C. C. Garner, J. W. Hell, *J. Biol. Chem.* **273**, 19518 (1998); C. Rongo, C. W. Whitfield, A. Rodal, S. K. Kim, J. M. Kaplan, *Cell* **94**, 751 (1998); J. H. Kim and R. L. Huganir, *Curr. Opin. Cell Biol.* **11**, 248 (1999); M. Wyszynski and M. Sheng, *Methods Enzymol.* **294**, 371 (1999); P. Li et al., *Nature Neurosci.* **2**, 972 (1999).

21. Single-letter abbreviations for the amino acid residues are as follows: A, Ala; C, Cys; D, Asp; E, Glu; F, Phe; G, Gly; H, His; I, Ile; K, Lys; L, Leu; M, Met; N, Asn; P, Pro; Q, Gln; R, Arg; S, Ser; T, Thr; V, Val; W, Trp; and Y, Tyr. X indicates any residue.

22. T. A. Benke, A. Luthi, J. T. Isaac, G. L. Collingridge, *Nature* **393**, 793 (1998); V. Derkach, A. Barria, T. R. Soderling, *Proc. Natl. Acad. Sci. U.S.A.* **96**, 3269 (1999).

23. It is possible that phosphorylation of GluR1 at Ser⁸³¹ and another protein are both necessary for AMPA-R delivery. In this case, S831A may mimic phosphorylation of Ser⁸³¹, possibly by preventing a protein-protein interaction mediated by the hydroxyl group of Ser. The marked synaptic potentiation seen in cells expressing GluR1(S831A)-GFP-IRES-tCaMKII supports this view.

24. The phosphorylation of Thr⁸⁸⁷ by CaMKII is not likely because, in the case of GluR1, phosphorylation stimulated by either neuronal activity or CaMKII occurs exclusively on the Ser residue in both endogenous and recombinant protein, but not on the Thr residue [C. Blackstone et al., *J. Neurosci.* **14**, 7585 (1994); A. Barria, thesis, Vollum Institute, Portland, OR (1998)].

25. The depression by GluR1(T887A)-GFP of transmission may be explained in the following manner. Normally, there is a pool of GluR1-containing AMPA-Rs outside the synapse. Upon activation of CaMKII-dependent plasticity, these receptors are incorporated into a delivery pathway in which PDZ proteins play a critical role. This delivery process may contain elements used in a separate, constitutive delivery process; such a process appears to act on AMPA-Rs containing GluR2 and requires N-ethylmaleimide-

sensitive fusion protein (NSF). The mutant receptor appears to be recruited, upon CaMKII activation or LTP, into an interaction site where it can block this constitutive process; the time-course of its effects on transmission is similar to the effect of peptides that block the interaction between GluR2 and NSF [A. Nishimune et al., *Neuron* **21**, 87 (1998); P. Osten et al., *Neuron* **21**, 99 (1998); I. Song et al., *Neuron* **21**, 393 (1998); J. Noel et al., *Neuron* **23**, 365 (1999)].

26. Supplemental material is available at www.sciencemag.org/feature/data/1046986.shl

27. We thank C. Sano for help in DNA construction, N.

Dawkins-Pisani for technical assistance, and H. Schulman, M. Hollmann, and S. F. Heineman for cDNA clones. Y.H. was supported by Japan Society for the Promotion of Science and Uehara Memorial Foundation, J.A.E. by Alzheimer Association and National Alliance for Research on Schizophrenia and Depression, and J.-C.P. by the Human Frontier Science Program Organization. This study was supported by NIH and the Mathers Foundation (to R.M).

11 November 1999; accepted 28 January 2000

Response of Schwann Cells to Action Potentials in Development

Beth Stevens and R. Douglas Fields*

Sensory axons become functional late in development when Schwann cells (SC) stop proliferating and differentiate into distinct phenotypes. We report that impulse activity in premyelinated axons can inhibit proliferation and differentiation of SCs. This neuron-glia signaling is mediated by adenosine triphosphate acting through P2 receptors on SCs and intracellular signaling pathways involving Ca²⁺, Ca²⁺/calmodulin kinase, mitogen-activated protein kinase, cyclic adenosine 3',5'-monophosphate response element binding protein, and expression of *c-fos* and *Krox-24*. Adenosine triphosphate arrests maturation of SCs in an immature morphological stage and prevents expression of O4, myelin basic protein, and the formation of myelin. Through this mechanism, functional activity in the developing nervous system could delay terminal differentiation of SCs until exposure to appropriate axon-derived signals.

Neural impulse activity has a critical influence on development of the nervous system at late stages of prenatal development and early postnatal life. By regulating neuronal survival, outgrowth, synaptic organization, and gene expression, impulse activity in developing neural circuits helps tailor nervous system structure in accordance with functional requirements (1). Much less is known regarding possible activity-dependent regulation of nonneuronal cells (glia) during development. These cells provide essential structural and functional support for developing and adult neurons and undergo marked changes in proliferation, lineage progression, and differentiation during late stages of development when neural impulse activity could provide an instructive influence. The objective of the present study was to determine whether SCs can detect impulses from premyelinated axons and, if so, to identify the signaling pathways responsible and their functional consequences.

Time-lapse confocal microscopy was used to monitor changes in intracellular Ca²⁺ in

SCs in response to electrical stimulation of dorsal root ganglion (DRG) neurons (2). Calcium imaging has been used to detect activity-dependent axon-SC communication in the adult nervous system at the nodes of Ranvier (3) and synaptic terminals (4) in association with K⁺ buffering and neurotransmitter secretion. However, it is not known whether SCs can detect impulse activity in extrasynaptic regions and in premyelinated axons before formation of nodes of Ranvier. This was investigated by culturing SCs (5) on DRG (6) axons in a preparation equipped with stimulating electrodes (7). Calcium levels increased immediately in neurons in response to action potential firing and activation of voltage-sensitive Ca²⁺ channels. Fifteen to 150 s after stimulation at 10 Hz (Fig. 1, A and B), intracellular Ca²⁺ increased to high levels in multiple SCs associated with the axons. The Ca²⁺ response in SCs varied proportionately with stimuli between 1 and 10 Hz and could be elicited repeatedly by electrical stimulation delivered several minutes after Ca²⁺ recovery to basal levels (Fig. 1B) (8).

The delay between the neuronal and the SC response suggests involvement of a soluble signaling molecule released from nonsynaptic regions because synapses do not form in pure DRG cultures (9). The evidence suggests that the Ca²⁺ response of SCs is mediated by adenosine triphosphate (ATP) re-

Laboratory of Developmental Neurobiology, National Institutes of Health, National Institute of Child Health and Human Development, Building 49, Room 5A38, 49 Convent Drive, Bethesda, MD 20892, USA.

*To whom correspondence should be addressed. E-mail: fields@helix.nih.gov